

# Improving Emphysema Diagnosis Accuracy through Deep Convolutional Neural Networks: Analysis of Chest X-ray and Chest CT Scan Images

Ramadoss Ramalingam<sup>1</sup>, Vimala Chinnaiyan<sup>2\*</sup>

<sup>1</sup>Department of Electronics and Communication Engineering, College of Engineering and Technology, SRM Institute of Science and Technology, Kattankulathur, 603203, Chengalpattu Dt, Tamil Nadu, India.

<sup>1</sup>Email: rr5606@srmist.edu.in

<sup>2\*</sup>Department of Electronics and Communication Engineering, College of Engineering and Technology, SRM Institute of Science and Technology, Kattankulathur- 603203, Chengalpattu Dt, Tamil Nadu, India.

<sup>2\*</sup>Email: vimalac@srmist.edu.in

## ARTICLE INFO

## ABSTRACT

Received: 12 Nov 2024

Revised: 25 Dec 2024

Accepted: 20 Jan 2025

Chronic obstructive pulmonary disease (COPD) is a complex respiratory condition involving various lung parenchymal anomalies. The major aim of this research is to enhance the diagnostic accuracy of Emphysema, a type of COPD, by leveraging Convolutional Neural Networks (CNNs) applied to Chest CT scan and Chest X-ray (CXR) images. The proposed CNN method consists of nine convolutional layers, each followed by batch normalization (BN), ReLU activation, and eight max-pooling layers, along with two strategically placed dropout layers to prevent overfitting. The model further includes fully connected, SoftMax, and classification layers, encompassing 15.7 million trainable parameters. The primary objective is to minimize false negatives, where Emphysema patients are misclassified as healthy while also maintaining low false positive and false negative rates, crucial for healthcare applications. On the benchmark dataset, the model achieved a validation accuracy of 97.01%. When applied to the real-time database from SRM Medical College Hospital & Research Centre, the model's performance improved significantly, reaching a validation accuracy of 99.05%. The study demonstrates the effectiveness of deep CNNs in enhancing Emphysema diagnosis accuracy by analyzing Chest CT and X-ray images. The model's ability to reduce false negatives is particularly impactful for early COPD detection, offering significant potential for improving patient outcomes in healthcare settings.

**Keywords:** Convolutional Neural Network (CNN), Chronic obstructive pulmonary disease (COPD), Deep Learning, Emphysema.

## INTRODUCTION

According to the World Economic Forum (WEF), the worldwide cost of chronic illnesses in 2030 might exceed 47 trillion dollars [1]. In general, COPD exacerbations are difficult to diagnose in medical field [2]. So, COPD is a leading cause of death globally. It is estimated that more than 70% of COPD patients are misdiagnosed. Emphysema is a significant part of COPD. It occurs when the lung parenchyma is damaged [3]. Emphysema is often diagnosed in advanced stages and is a potential element for pulmonary malignancy. COPD and Emphysema are known to increase lung cancer risk [4].

Early detection of emphysema is very essential. Emphysema is "abnormal, permanent enlargement of the airspaces in the terminal bronchioles, followed by degeneration without fibrosis of alveolar walls and loss of elasticity of the lung parenchyma" [5]. COPD is when the airflow to the lungs becomes increasingly restricted over time and cannot reopen. Many conditions might cause this limitation, including alveolar wall degeneration and elasticity loss. Emphysema is one such condition [6]. Low attenuation patches on computed tomography (CT) scans indicate the presence of Emphysema (LAA). With the automatic quantification and detection of Emphysema, clinical routines assessing COPD can be more objective and reliable in their results. Emphysema is presently assessed physically, which is inefficient, inaccurate, and subject to observer variability [7]. The commonly used approaches for automatically analyzing Emphysema are based upon density calculations [8-10]. Both radiographically and clinically,

the diagnosis of emphysema is essential [11]. Radiologists and physicians may reduce observational errors and false negative rates when evaluating medical images by employing software called CAD, which evaluates diseases using medical images [12].

Current approaches to diagnosis include a clinical examination, pulmonary function tests, chest X-rays and CT scans. Among these, CT scan is needed to scale the severity of emphysema, but it is rarely utilized to diagnose and treat patients with COPD. [13]. Instead, X-ray images are used. Collapsed lungs may be harder in people with severe emphysema because lung function is already reduced. This is an unusual yet dangerous incident. Emphysema affects the heart because it raises pressure in the arteries that connect the heart and lungs [14-15]. The objective of this investigation is to create a categorization framework for identifying emphysema. The convolutional neural networks (CNNs) are powerful image-understanding approaches.

Several articles have published on the application of image processing, machine learning, and deep learning to diagnose emphysema. The current developments enable the detection, measurement and classification of patterns in medical images [16]. Researchers suggest a CNN model with 9 convolutional stages in this article: a nine-batch normalization level, a nine-rectified linear unit (ReLU) layer, an eight-max pooling layer, and two dropout layers: 2 completely linked layers, one SoftMax layer, and one classification layer. The following parts discuss numerous literature surveys and related works of the preprocessing stage and classification process, specifically the CNN model to detect pulmonary emphysema disease.

With respect to the quality of chest x-ray picture, critical information may be missed. As a result, picture preprocessing is used to increase image clarity [17]. In [18], an upgraded computer-assisted deep-learning technique for 2021 is proposed. The image is first pre-processed using histogram levelling and median filtering. The first step is to pre-process the image, which is done by histogram levelling and median filtration. Due to advances in CNN technology, image classification, and detection have significant gains. Using CNN instead of manually designing, extracting and selecting features, CNN can understand representative features from data at different levels (which are time-consuming and error-prone). A deep learning system for identifying mortality-related impairment in emphysema characteristics was suggested by [19]. Emphysema is categorized using Fleischer parameters, CNN, and cognitive modules, which are adequately conditioned. In [20] suggested a 3D CNN to classify COPD and emphysema. The CNN classifies raw emphysema images well presented by [21]. This is validated by the 84.25 percent accuracy attained without preprocessing. In [22] suggested a deep-learning strategy for the categorization of emphysema under multi-scale ResNet along two channels of original CT imagery. In [23] suggested a CNN framework that effectively collects information and produces categorization from unprocessed pictures. A novel multi-scale rotation-invariant (MRCNN) framework have presented for categorizing 5 lung tissue morphologies [24] In [25] ILD patterns can be classified using CNN. Additional methods are used to classify COPD. CNN techniques may improve Emphysema risk models, according to the researchers, in the absence of visual assessment of the lung parenchyma or PFTs (pulmonary function tests). Emphysema can be detected or distinguished in CT images using several existing machine-learning methods, although these approaches have not well investigated. It's still unclear how deep neural networks determine the best way to classify pictures based on their feature layers. The gradient-weighted class activation mapping from a CNN creates visual explanations. It enables viewers to see the areas focused on by CNN, which may be able to overcome this problem [26]. The motivation behind our proposed method is to elevate diagnostic accuracy within the context of Emphysema, a subtype of COPD. The primary objective is to enhance the precision of Emphysema diagnosis. This motivation arises from the recognition that Emphysema, much like other COPD subtypes, presents intricate respiratory challenges characterized by varying degrees of lung parenchymal abnormalities. Traditional diagnostic protocols rely on pulmonary function testing, Chest X-ray and CT scan.

The proposed method leverages Convolutional Neural Networks (CNNs) to analyze both Chest X-ray and Chest CT scan images, and it is motivated by the potential to achieve more precise and efficient diagnostic outcomes. By harnessing the capabilities of deep learning and computational methods, this research seeks to minimize errors in Emphysema diagnosis, addressing both false negatives (cases where Emphysema patients might be incorrectly identified as healthy individuals) and false positives (cases where healthy individuals might be incorrectly identified as Emphysema patients). This dual focus on reducing diagnostic errors has significant implications in healthcare, as it can lead to earlier intervention and improved patient outcomes.

Remaining paper is designed as: Section II describes the dataset as well as the proposed CNN model built for pulmonary emphysema diagnosis. Section III exemplifies the results. Section IV concludes this paper.

## METHODS

In this research, the prediction of Emphysema is a great challenge as it may increase the risk to the patient's life. In the healthcare industry, medical image processing and analysis are essential when images are estimated to account for at least 90% of all medical data.

The major contributions of this research are:

- An imaging system is designed for data storage, categorizing images into two distinct subfolders based on their class names. Specifically, images of infected x-rays along chest CT scans systematically organized within the "Emphysema" subdirectory, while those depicting uninfected x-rays and chest CT scans are stored in the "normal" subfolder.
- Subsequently, the dataset is separated into discrete sets for training and testing with 80 percent allocated to training and 20 percent for testing. This partitioning is essential for ensuring the accuracy of the proposed approach.
- In addition, the data augmentation techniques are employed and execute image preprocessing to enhance the quality and diversity of dataset.
- Utilize the fine-tuning of hyperparameters to enhance the model's efficacy. A two distinct imaging models are used: chest X-ray and CT scans. The experimental analysis has yielded positive test results, confirming their effectiveness in the diagnosis of emphysema. The research also presents comparative testing outcomes, providing valuable insights into the performance of these imaging modalities for emphysema detection.

### 2.1 Datasets

This research makes use of datasets for the analysis of Emphysema. Table 1 gives the benchmark dataset. The datasets are created using chest X-rays collected from <https://doi.org/10.5281/zenodo.6373392> [27] together with National Institute of Health Clinical Center. In contrast, the normal x-ray database can be found in Kaggle and RSNA. In which, 6038 imageries are considered for training, 1510 imageries are considered for testing. Table 2 tabulates the real-time dataset obtained through manual collection at SRM Medical College Hospital with Research Centre. The dataset comprises 976 samples, which divided into 780 for training and 196 for testing purposes. Table 3 illustrates the effect of augmenting the sample size, resulting in an expanded dataset of 19,520 samples. Among these, 15,616 are allocated for training, while 3,904 for testing.

**Table 1:** Preparation of Benchmark datasets

Samples	Train Images	Test images	Total
Emphysema	3019	755	3774
Normal	3019	755	3774
Total	6038	1510	7548

**Table 2:** Preparation of Manual datasets

Samples	Train Images	Test images	Total
Emphysema	390	98	488
Normal	390	98	488
Total	780	196	976

**Table 3:** Preparation of Manual datasets after augmentation

Samples	Train Images	Test images	Total
Emphysema	7808	1952	9760
Normal	7808	1952	9760
Total	15616	3904	19520

## 2.2 Data Augmentation

An image data augmenter contains several preprocessing parameters for picture supplementation, such as resizing, orientation, and indication ability. The data augmentation is used to improve the categorization of any chest X-ray image. It replaces the original batch of pictures with a new group of images that randomly modified. Augmentation operations are employed to generate new variations of the original images. This involved defining cropping parameters, specifically cropHeight and cropWidth, which determine the desired height and width for cropping images during the augmentation process. Furthermore, transformations like rotation, mirroring (reflection), and shearing are applied to enhance the dataset's diversity. For instance, the 'RandRotation' property is utilized to specify a random rotation range spanning from -5 to 5 degrees. Additionally, 'RandXReflection' and 'RandYReflection' properties are configured with a value of 1, signifying that horizontal and vertical reflections (mirroring) could be randomly applied. Finally, the 'RandXShear' and 'RandYShear' properties dictated random shearing within the horizontal and vertical dimensions. These transformations are randomly applied to each image, and the resulting augmented images are saved in a separate folder. To maximize the size and diversity of training dataset and increase the performance of machine learning models, computer vision and machine learning practitioners frequently employ this data augmentation technique.

## 2.3 Image preprocessing

Preprocessing improves image quality and image attributes for further processing. The median filter is used for hue equalization and distortion suppression. Smoothing is accomplished via a Wiener filter. Fig 1 depicts the proposed fusion approach for medical image denoising.

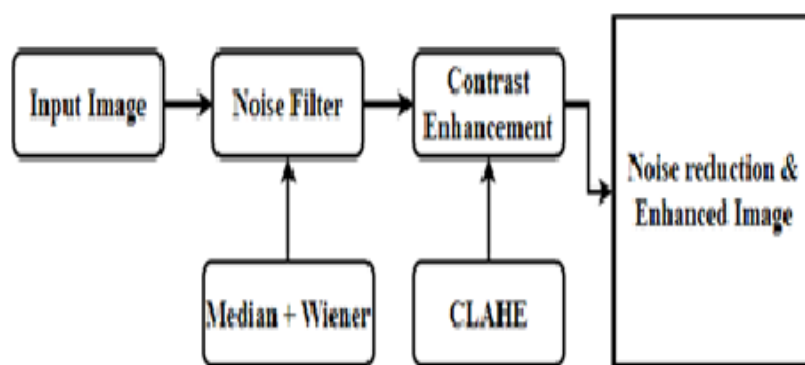


Fig 1: Preprocessing stage

### 2.3.1 Median Filter

A non-linear technique called the median filter is used to reduce image noise. The value of each pixel is changed to reflect the nearby median value. Mathematically, it is expressed in equation (1),

$$I_{median}(x, y) = \text{median}\{I(x + i, y + j) \text{ for } -k \leq i \leq k, -k \leq j \leq k\} \quad (1)$$

In this equation,  $I$  represents input image,  $I_{\text{median}}$  represents the image after median filtering, and  $(x,y)$  denote pixel coordinates. The size of the neighborhood is computed by the kernel size (e.g.,  $2k+1$ ).

### 2.3.2 Wiener filter

The Wiener filter, typically applied in the frequency domain, is utilized to enhance images and reduce noise. It can be mathematically expressed as:

$$G(l,m) = \frac{H^*(l,m)}{|H(l,m)|^2 + \frac{S_n(l,m)}{S_f(l,m)}} F(l,m) \quad (2)$$

here:

- $G(l,m)$  refers Fourier transform of the enhanced image.
- $H^*(l,m)$  implicates complex conjugate of the Fourier transform to the Point Spread Function (PSF).
- $|H(l,m)|^2$  represents the squared magnitude of the PSF.
- $S_n(l,m)$  implies power spectral density for noise.
- $S_f(l,m)$  implies power spectral density for actual image.

It is also known as the Least Square Error Filter and the Minimum Mean Square Error Filter. It eliminates additive noise while simultaneously inverting blurring. In the process of inverse filtering and noise smoothing, it minimizes the global mean square error. Because of this, hybrid filters lead to better image quality, which makes it easier for any research method to produce valuable results. This study uses a combination of median and Wiener filters (fusion filters) for noise removal.

### 2.3.3 CLAHE

Enhancing the X-ray images quality involves the application of Contrast-limited adaptive histogram equalization (CLAHE) techniques [28]. On medical imaging, CLAHE results were excellent. Contrast enhancement is handled via the adaptive histogram equalization (AHE) method. It functions by employing "tiles," which are tiny fragments of an image as opposed to the entire image [29]. CLAHE is employed to enhance local contrast within images. It operates in the spatial domain and is specified in equation (3):

$$I_{\text{CLAHE}}(l,m) = \text{CLAHE}(I(l,m)) \quad (3)$$

here,  $I_{\text{CLAHE}}$  represents the image after applying CLAHE,  $I$  is the input image, and  $(l,m)$  denote pixel coordinates.

To ensure continuity between these operations:

- Begin by applying the median filter to the input image, resulting in  $I_{\text{median}}$ .
- Subsequently, apply the Wiener filter to  $I_{\text{median}}$ , yielding  $G(l,m)$  at the frequency domain.
- Perform inverse Fourier transform on  $G(l,m)$  to obtain the enhanced image in the spatial domain.
- Finally, apply CLAHE to the enhanced image from the previous step, leading to  $I_{\text{CLAHE}}$ .

## 2.4 Convolutional Neural Networks (CNN)

A CNN or ConvNet integrates acquired characteristics with source information and includes 2D convolutional levels, making it perfect for analyzing two-dimensional pictures.

CNN can be divided into two broad categories, such as "feature learning" and "classification," as illustrated in Fig 2. The network pictures are utilized to recover elements, and the impulses derived from the recovered features are used to categorize the pictures. Classification neural networks that operate based on image features generate the output.

The neural network for feature extraction comprises 2D convolutional, BN, ReLU, max pooling 2D layers. These four layers use repetitively, which means different blocks of these four layers in between input and output. It contains nine blocks. The final layers include completely linked Soft max, and categorization layers. Following this, the output is obtained in different categories. The different layers of CNN are explained below.

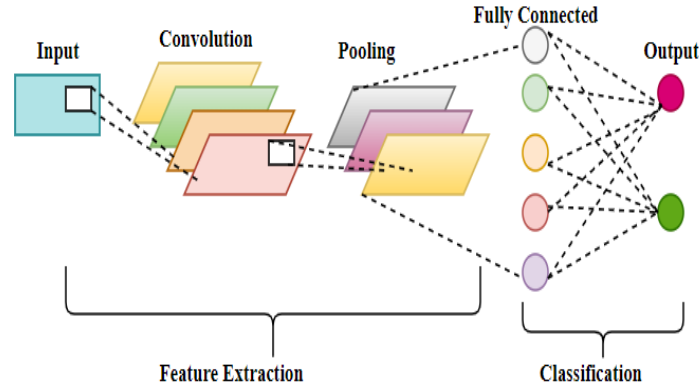


**Fig 2:** Basic CNN model

#### 2.4.1 Layers of a CNN

(i) Image Input Layer: The image size is specified on this layer

(ii) Convolutional Layer: It is the primary layer in charge of feature extraction. Here, a convolution operation is carried out and is labelled in equation (4),

$$O_{ij} = \sum_{m=1}^M \sum_{n=1}^N I_{(i-m)(j-n)} \cdot K_{mn} \quad (4)$$

here

- $O_{ij}$  indicates the value located on  $(i, j)$  position within the created feature map.
- $I_{(i-m)(j-n)}$  denotes input value of  $(i-m, j-n)$  position.
- $K_{mn}$  signifies weight in the convolutional kernel at position  $(m, n)$ .
- $M$  and  $N$  implies dimensions of the kernel.

(iii) Batch normalization layer: normalizing the activations and gradients makes it easier to figure out the best way to train a network. It also speeds up training and makes the network less sensitive to how it was set up when it was first trained.

(iv) ReLU Layer: ReLU is the most often utilized function for CNN since it requires less computing time and performs quicker than the other two functions, such as sigmoid and tan hyperbolic. In the Activation Layer, an elementwise ReLU function is applied to each element of the input feature map:

$$A_{ij} = \max(0, I_{ij}) \quad (5)$$

where:



$A_{ij}$  represents the value after applying ReLU to the input  $I_{ij}$

(v) Max Pooling Layer: The down sampling method reduces the feature map's size and eliminates any unnecessary spatial data. The Pooling Layer, often Max Pooling, down samples the input by choosing maximal value in a local window:

$$P_{fg} = \max(I_{(f.Qx):(f.Qx+Kx-1),(g.Qy):(g.Qy+Ky-1)}) \quad (6)$$

where:

$P_{fg}$  is the output value at position (f, g).

$I_{(f.Sx):(f.Sx+Kx-1),(g.Sy):(g.Sy+Ky-1)}$  represents the local window of the input.

$Qx$  and  $Qy$  are the strides in x and y directions.

$Kx$  and  $Ky$  are the dimensions of the pooling window.

(vi) Fully Connected Layer: CNN's structure includes a Fully Connected Layer (FCL). The objective of the FCL is to categorize detected characteristics into categories and also learn how to correlate observed features with a certain label. FCL is similar to an artificial neural network in which every neuron is linked with all other neurons in the layer next and previous.

At FCL, a matrix multiplication is performed followed by an addition of bias:

$$O_i = \sum_{j=1}^N I_j \cdot W_{ij} + B_i \quad (7)$$

where:

The output of neuron i is denoted as  $O_i$

$I_j$  is the input from the previous layer's neuron j.

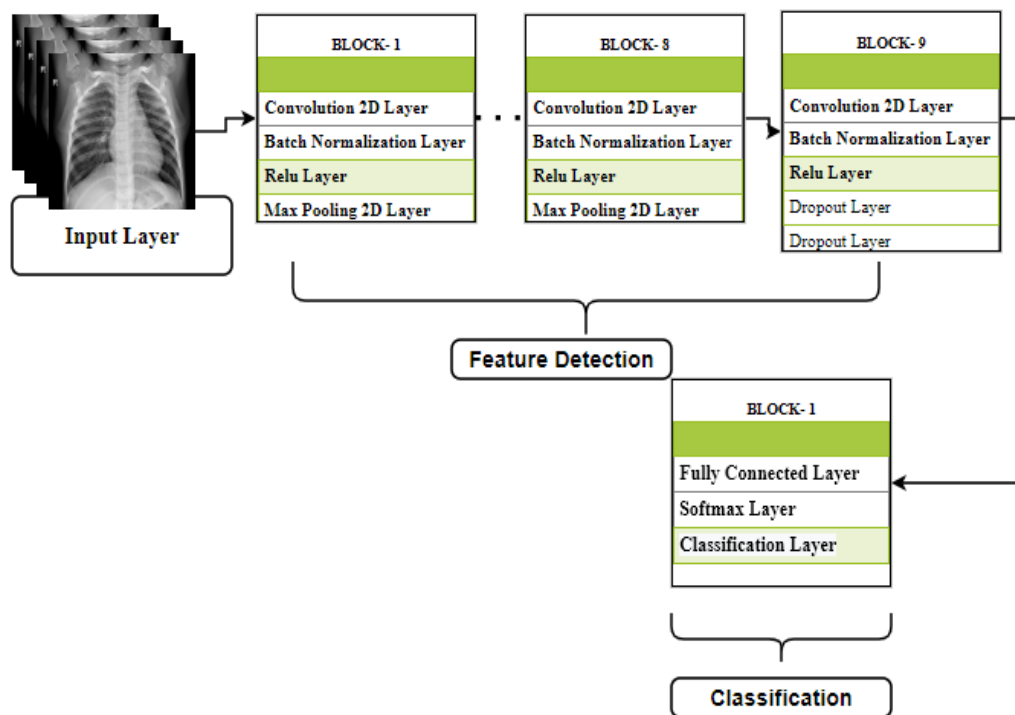
$W_{ij}$  represents the weight linked to the connection between neuron j and neuron i.

$B_i$  is the bias term for neuron i.

(vii) SoftMax layer: The SoftMax initiation mechanism generalizes the completely linked layer's result. Additionally, it generates affirmative data that sum up to 1, which can be utilized by the classification model as probabilities for classification.

(viii) Classification Layer: This layer sends every input to the appropriate equally distinct categories and calculates the losses using the likelihood supplied by the SoftMax initiation feature.

A new 41-layer CNN model is developed, as shown in Fig 3. First, the input image layer is fed to several operations, including convolution, max pooling, etc. The same technique yields distinct layers, the final of which is used for classification using the SoftMax function. The proposed convolutional neural network used in this paper consists of 41 layers represented in Table 4.

**Fig 3:** Proposed CNN model

The proposed model consists of multiple layers, encompassing convolutional layers, batch normalization (BN) layers, Rectified Linear Unit (ReLU) activation layers, max-pooling (MP) layers, dropout layers, fully connected layers (FCL), a SoftMax layer, and a classification layer. It's crucial to highlight that the architecture of the model can be customized to manage its complexity and performance attributes.

**Table 4:** Layers of CNN

S.No	Layer Type	Number of Filters	Filter Size	Stride	Padding	Number of Learnable
1	Image Input					0
2	2-D Convolution	8	3 X 3	[1,1]	Same	224
3	BN					16
4	Rectified Linear Unit					0
5	2-D Max Pooling		2 X 2	[2,2]	[0,0,0,0]	0
6	2-D Convolution	16	3 X 3	[1,1]	Same	1168
7	BN					32
8	Rectified Linear Unit					0
9	2-D Max Pooling		2 X 2	[2,2]	[0,0,0,0]	0
10	2-D Convolution	32	3 X 3	[1,1]	Same	4640
11	BN					64
12	Rectified Linear Unit					0



13	2-D Max Pooling		2 X 2	[2,2]	[0,0,0,0]	0
14	2-D Convolution	64	3 X 3	[1,1]	Same	18496
15	BN					128
16	Rectified Linear Unit					0
17	2-D Max Pooling		2 X 2	[2,2]	[0,0,0,0]	0
18	2-D Convolution	128	3 X 3	[1,1]	Same	73856
19	BN					256
20	Rectified Linear Unit					0
21	2-D Max Pooling		2 X 2	[2,2]	[0,0,0,0]	0
22	2-D Convolution	256	3 X 3	[1,1]	Same	295168
23	BN					512
24	Rectified Linear Unit					0
25	2-D Max Pooling		2 X 2	[2,2]	[0,0,0,0]	0
26	2-D Convolution	512	3 X 3	[1,1]	Same	1180160
27	BN					1024
28	Rectified Linear Unit					0
29	2-D Max Pooling		2 X 2	[2,2]	[0,0,0,0]	0
30	2-D Convolution	1024	3 X 3	[1,1]	Same	4719616
31	BN					2048
32	Rectified Linear Unit					0
33	2-D Max Pooling		2 X 2	[2,2]	[0,0,0,0]	0
34	2-D Convolution	1024	3 X 3	[1,1]	Same	9438208
35	BN					2048
36	Rectified Linear Unit					0
37	Dropout					0
38	Dropout					0
39	Fully Connected					2050
40	SoftMax					0
41	Classification Output					0

Table 5: Mini-Batch Options

Parameters	Value (Benchmark dataset)	Value (Manual dataset)
MaxEpochs	100	10
MiniBatchSize	128	128
Shuffle	'every-epoch'	'once'

**Table 6:** Training Options for ADAM

Parameters	Value (Benchmark dataset)	Value (Manual dataset)
Optimizer	Adam (adaptive moment estimation)	Adam
Learning rate (LR)	4.0000e-04	1.0000e-03
L2 regularization factor	1.0000e-04	1.0000e-04
Size of mini-batch	128	128

**Table 7:** Validation Options

Parameters	Value (Benchmark dataset)	Value (Manual dataset)
Validation Data	1510	196 3904
Validation Frequency	30	35 35
Validation Patience	Inf	5 5
Output Network	'last-iteration'	'last-iteration' 'last-iteration'

## RESULTS



**Fig 4:** Preprocessing Result



**Figure 5:** Visualize all Layers

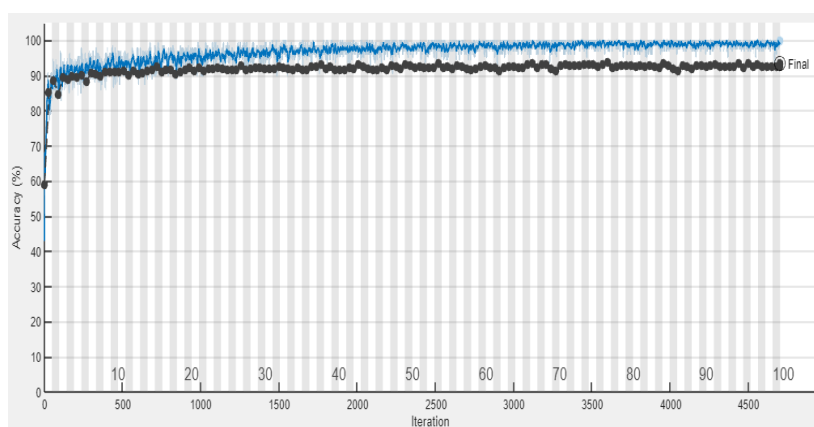


**Figure 6:** Training with validation Process (Accuracy vs. Iteration)-Benchmark dataset

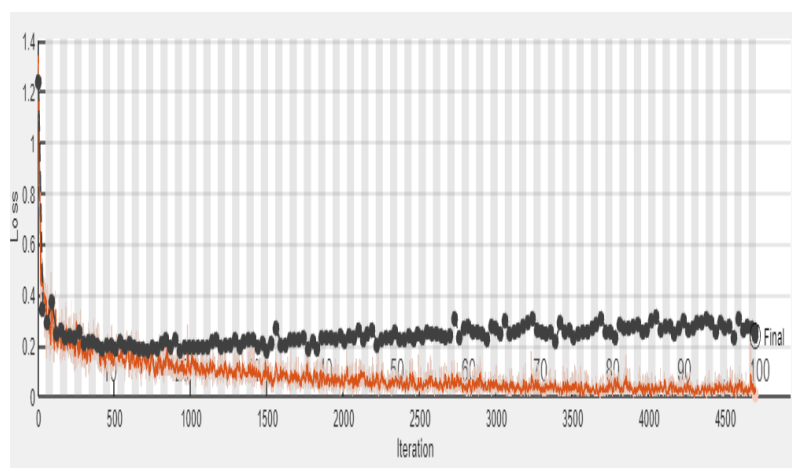


**Figure 7:** Training with validation Process (Loss vs. Iteration) for the Benchmark dataset.

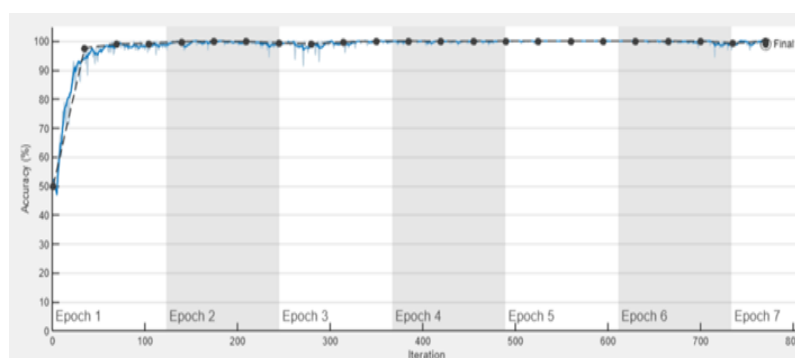


**Figure 8:** Training with validation Process (Accuracy vs. Iteration)-Manual database

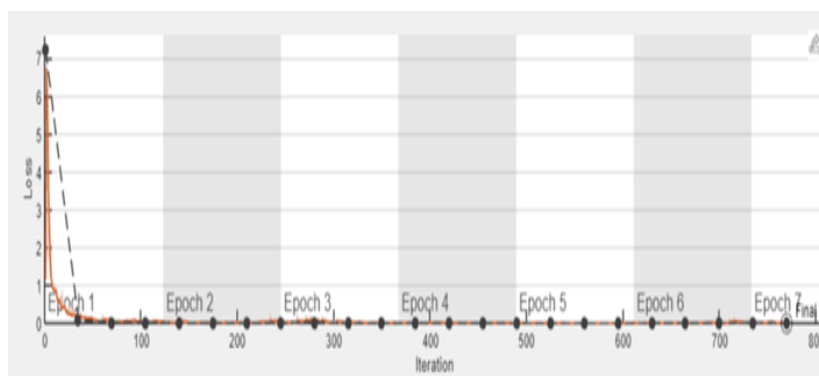


**Figure 9:** Training and validation Procedure (Loss vs. Iteration)-Manual dataset

The red and black lines in Figures 4, 5 and 6 show the training and validation processes, respectively. Figures 7, 8 and 9 depict the testing procedure to determine if it predicts correctly or incorrectly. The preprocessing methods such as the Fusion filter (median plus Wiener) are applied to the input image. After preprocessing, the pre-processed image is entered into the classification step using the proposed CNN model, and the expected score is one.

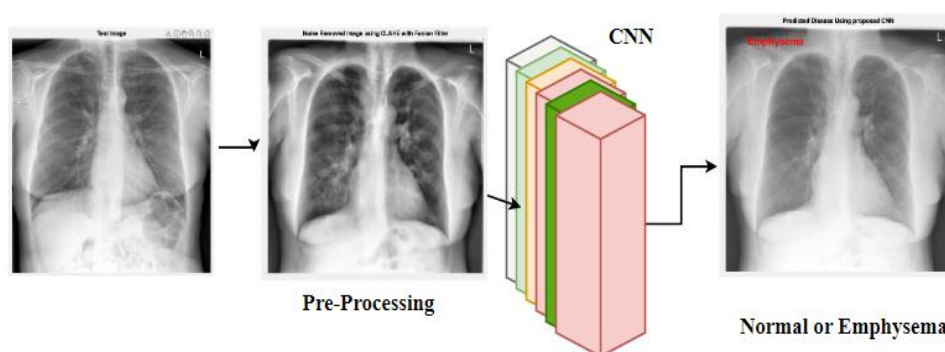


Fig 10: Testing processes

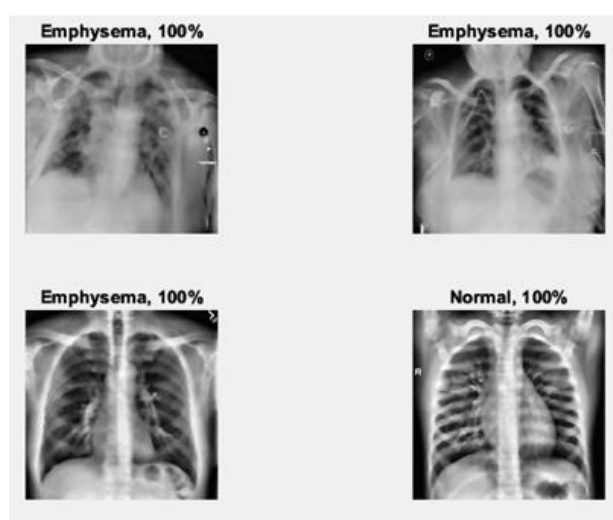


Fig 11: CNN model classified result

### 3.1 Performance Metrics

The performance metrics that are considered for analysis are given in this section. The most critical parameter considered is accuracy. The classifiers can be used to produce hypothesized class labels for each sample of a test perform. An estimate is either correct or incorrect for each test example. The classifier's accuracy can be determined by separating a count of test instances by a number of proper decisions made by the classifier.

- Accuracy: It is possible to calculate the accuracy of a dataset of correct classifications by dividing the total dataset by the overall classifications in the dataset.
- Precision is the ratio between the volume of properly categorized information and the cumulative value of accurately projected categorized information in a specific sample size.
- Recall: The recall statistic is the ratio among the volume of precisely categorized information and the total volume of accurately categorized information.
- F1-Score: The uniform average of the precision and recall values.

TPR and TNR are substantial in this instance, whereas FPR and FNR are minimal. As a result, the proposed methodology is neither underfitting nor overfitting. The precision and recall should always be high.

### 3.2 Confusion Matrix

This is computed using the NxN confusion matrix, where N represents total number of target classes. As seen in Figure 10, 11 and 12, the matrix compares actual values to machine-learning model predictions. This matrix may be

used to determine the classification error and prediction accuracy in the confusion matrix. In the image below, there are two things to note. Predicted value - the values predicted by the model. Actual Value-The values discovered in a dataset.

		Actual Values		
		Emphysema	Normal	
Predicted Values	Emphysema	1952 TP	0 FP	100% PPV
	Normal	37 FN	1915 TN	98.1% NPV
		98.13% TPR	100% TNR	99.05% ACC

(a)




		Actual Values		
		Emphysema	Normal	
Predicted Values	Emphysema	97 TP	1 FP	98.97% PPV
	Normal	2 FN	96 TN	97.95% NPV
		97.97% TPR	98.96% TNR	98.47% ACC

(b)

		Actual Values		
		Emphysema	Normal	
Predicted Values	Emphysema	734 TP	21 FP	97.21% PPV
	Normal	24 FN	731 TN	96.82% NPV
		96.83% TPR	97.20% TNR	97.01% ACC

(c)

**Fig 12:** Confusion Matrix (a) Testing samples (n=3094)-Manual dataset (b) Testing samples (n=196)-Manual dataset (c) Testing samples (n=1510)- Benchmark dataset

Test Image	Pre-processed Image using fusion filter with CLAHE	Predicted disease using proposed CNN model
		

**Fig 13:** Testing Process with a Manual Dataset

**Table 8:** Performance metrics for the proposed model

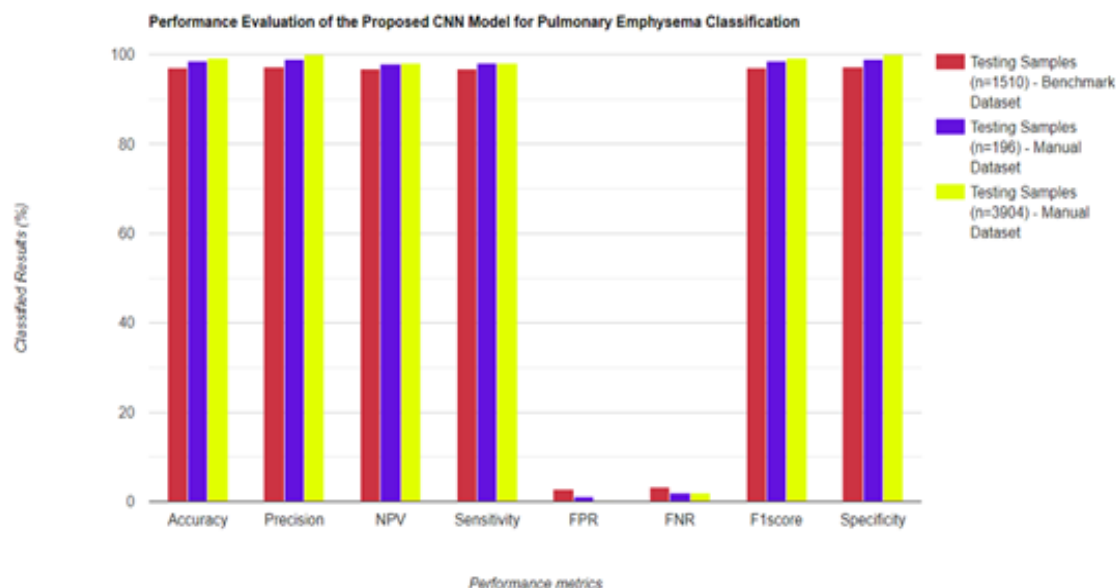
Number of instances	Accuracy (%)	Precision / PPV (%)	NPV (%)	Sensitivity/Recall /TPR (%)	Specificity / TNR (%)	FPR (%)	FNR (%)	F1-score (%)
Benchmark dataset- Chest X-ray								
1510	97.01	97.21	96.82	96.83	97.20	2.79	3.16	97.01
Manual dataset-Chest CT-Before augmentation								
196	98.47	98.97	97.95	97.97	98.96	1.03	2.02	98.46
Manual dataset-Chest CT- After augmentation								



---

3904	99.05	100	98.1	98.13	100	0	1.86	99.05
------	-------	-----	------	-------	-----	---	------	-------

---

**Fig 14;** Pulmonary Emphysema Classification Results Using the Proposed CNN Model**Table 9:** Comparison between the suggested approach and the other CNN

Model	Method used	Dataset Types	Classification Accuracy	Disease
Karabulut and Ibrikci (2015)	CNN-2 layer	168 patches from 115 HRCT	84.25 %	Emphysema
Peng et al., (2020)	Multi-scale residual network	HRCT-91	93.74%	Emphysema
X.Pei[21]	CNN	HRCT	92.54%	Emphysema
Wang et al., (2017)	Multiscale Rotation-Invariant CNN	HRCT	73.62%	5 lung tissues
Anthimopoulos et al., (2016)	CNN-5 layer	120 CT scans	85.61%	ILD's
Proposed model	Proposed CNN-41layer	X-ray-7548	97.01%	Emphysema
Proposed model	Proposed CNN-41layer	3094- HRCT	99.05%	Emphysema

The comprehensive performance evaluation of our developed CNN model, compared to an existing model, is displayed in Table 5, 6 and 7. Additionally, Table 8 and 9 provides performance Fig 13 and 14 metrics for the proposed model on the testing dataset. The CNN model we introduced demonstrated satisfactory performance on both real-time and benchmark datasets.

## DISCUSSION

This work significantly advances the application of deep learning, particularly CNNs, for diagnosing Emphysema

using Chest CT and X-ray images, offering notable improvements over existing models. While previous research highlights the potential of CNNs for medical image analysis, our model's ability to achieve high diagnostic accuracy across multiple modalities and minimize false negatives represents a crucial step forward. The 99.05% validation accuracy on real-world clinical data, compared to benchmark datasets, underscores its strong generalizability, which is often a challenge in healthcare AI applications. By focusing on architectural strategies, such as dropout layers to prevent overfitting and optimizing false negative rates, we enhance diagnostic reliability, addressing a key issue in COPD detection. However, the model's reliance on high-quality imaging limits its use in resource-constrained environments, and further evaluation across diverse populations is necessary to confirm its broader applicability. Despite these limitations, our research makes a meaningful contribution to literature by presenting a robust, real-time CNN-based solution for Emphysema diagnosis that enhances early identification and patient outcomes in COPD care.

### CONCLUSION

Emphysema is diagnosed using pulmonary function testing, imaging, and blood tests under CNN models. This paper used an emphysema dataset to train a classifier algorithm to predict emphysema detection. Here, the chest X-ray images used as input parameters for a CNN. The performance metrics of CNN have been found. This research has mainly focused on reducing diagnosis errors through rapid computer applications. The detection of emphysema is implemented by employing the efficient CNN method. This research work is expected to lay the foundation for automated emphysema lung disease identification and classification of the emphysema stage. When compared to other deep learning models, the proposed model attains precision of 97.21%, sensitivity of 96.83%, classification accuracy of 97.01%, specificity of 97.20%, TPR of 96.83%, TNR of 97.20%, FPR of 2.79%, FNR of 3.16%, and F1-score of 97.01%. Therefore, this model helps to boost classification sensitivity and decrease false-positive rates. The real-time database is obtained through SRM Medical College with Research Centre. The results show classification accuracy 99.05%, precision 100%, sensitivity 98.13%, specificity 100%, TPR 98.13%, TNR 100%, low FPR 0%, a minimal FNR 1.86%, and F1-score 99.05%.

### ACKNOWLEDGEMENT

The authors wish to prolong their appreciation to SRM Medical College Hospital & Research Centre, Kattankulathur-603203, Chengalpattu, Tamil Nadu, India. They also express their gratitude to the National Institutes of Health Clinical Center, Kaggle, and the Radiological Society of North America (RSNA) for their generous provision of the dataset.

### Author Contribution:

**Ramadoss Ramalingam**-(First Author) - *Conceptualization Methodology, Original draft preparation*

**Vimala Chinnaiyan** -(Corresponding Author) -*Supervision*

### REFERENCES

- [1] Kelland K. Chronic disease to cost \$47 trillion by 2030: WEF2011. [Online]. Available:<https://www.reuters.com/article/us-disease-chronic-costs-idUSTRE78H2IY20110918>
- [2] Kevin F, O'Neil M, MD. Chronic Obstructive Pulmonary Disease (COPD), 2021. [Online]. Available:<https://foundation.chestnet.org/lung-health-a-z/chronic-obstructive-pulmonary-disease-copd/>.
- [3] Barnes PJ, Shapiro SD, Pauwels RA. Chronic obstructive pulmonary disease: molecular and cellular mechanisms. *European Respiratory Journal*. 2003;22(4):672-88.
- [4] Hatt C, Galban C, Labaki W, Kazerooni E, Lynch D, Han M. Convolutional neural network based COPD and emphysema classifications are predictive of lung cancer diagnosis. In *International Workshop on Reconstruction and Analysis of Moving Body Organs 2018* (pp. 302-309). Cham: Springer International Publishing.
- [5] Pahal SS, Avula P. A Emphysema StatPearls [Internet] 2022. <https://www.ncbi.nlm.nih.gov/books/NBK482217/>.

- [6] Pino Peña I, Cheplygina V, Paschaloudi S, Vuust M, Carl J, Weinreich UM, Østergaard LR, de Bruijne M. Automatic emphysema detection using weakly labeled HRCT lung images. *PloS one*. 2018;13(10):e0205397.
- [7] Ginsburg SB, Lynch DA, Bowler RP, Schroeder JD. Automated texture-based quantification of centrilobular nodularity and centrilobular emphysema in chest CT images. *Academic Radiology*. 2012;19(10):1241-51.
- [8] Matsuoka S, Yamashiro T, Washko GR, Kurihara Y, Nakajima Y, Hatabu H. Quantitative CT assessment of chronic obstructive pulmonary disease. *Radiographics*. 2010;30(1):55-66.
- [9] Lynch DA, Newell JD. Quantitative imaging of COPD. *Journal of thoracic imaging*. 2009;24(3):189-94
- [10] Nakano Y, Muro S, Sakai H, Hirai T, Chin K, Tsukino M, Nishimura K, Itoh H, Paré PD, Hogg JC, Mishima M. Computed tomographic measurements of airway dimensions and emphysema in smokers: correlation with lung function. *American journal of respiratory and critical care medicine*. 2000;162(3):1102-8.
- [11] Foster Jr WL, Gimenez EI, Roubidoux MA, Sherrier RH, Shannon RH, Roggli VL, Pratt PC. The emphysemas: radiologic-pathologic correlations. *Radiographics*. 1993;13(2):311-28.
- [12] Alagirisamy M. Micro statistical descriptors for glaucoma diagnosis using neural networks. *International Journal of Advances in Signal and Image Sciences*. 2021;7(1):1-0
- [13] Campo MI, Pascau J, Estépar RS. Emphysema quantification on simulated X-rays through deep learning techniques. In 2018 IEEE 15th International Symposium on Biomedical Imaging (ISBI 2018) 2018 (pp. 273-276). IEEE.
- [14] Ramalingam R, Chinnaiyan V. Intelligent optimization-based pulmonary emphysema detection with adaptive multi-scale dilation assisted residual network with Bi-LSTM layer. *Biomedical Signal Processing and Control*. 2024; 88:105643.
- [15] Shajin FH, P S, Rajesh P, Nagoji Rao VK. Efficient framework for brain tumour classification using hierarchical deep learning neural network classifier. *Computer Methods in Biomechanics and Biomedical Engineering: Imaging & Visualization*. 2023;11(3):750-7.
- [16] Kieu ST, Bade A, Hijazi MH, Kolivand H. A survey of deep learning for lung disease detection on medical images: state-of-the-art, taxonomy, issues and future directions. *Journal of imaging*. 2020;6(12):131.
- [17] Singh D, Kumar V, Yadav V, Kaur M. Deep neural network-based screening model for COVID-19-infected patients using chest X-ray images. *International Journal of Pattern Recognition and Artificial Intelligence*. 2021; 35(03):2151004.
- [18] Mondal S, Sadhu AK, Dutta PK. Adaptive local ternary pattern on parameter optimized-faster region convolutional neural network for pulmonary emphysema diagnosis. *IEEE Access*. 2021;9:114135-52
- [19] Humphries SM, Notary AM, Centeno JP, Strand MJ, Crapo JD, Silverman EK, Lynch DA, Genetic Epidemiology of COPD (COPDGene) Investigators. Deep learning enables automatic classification of emphysema pattern at CT. *Radiology*. 2020;294(2):434-44.
- [20] Ahmed J, Vesal S, Durlak F, Kaergel R, Ravikumar N, Rémy-Jardin M, Maier A. COPD classification in CT images using a 3D convolutional neural network. In *Bildverarbeitung für die Medizin 2020: Algorithmen – Systeme – Anwendungen. Proceedings des Workshops vom 15. bis 17. März 2020 in Berlin 2020* (pp. 39-45). Springer Fachmedien Wiesbaden
- [21] Karabulut EM, Ibriki T. Emphysema discrimination from raw HRCT images by convolutional neural networks. In 2015 9th International Conference on Electrical and Electronics Engineering (ELECO) 2015 (pp. 705-708). IEEE
- [22] Peng L, Lin L, Hu H, Li H, Chen Q, Ling X, Wang D, Han X, Iwamoto Y, Chen YW. Classification and quantification of emphysema using a multi-scale residual network. *IEEE journal of biomedical and health informatics*. 2019; 23(6):2526-36.
- [23] Peng L, Lin L, Hu H, Zhang Q, Li H, Chen Q, Wang D, Han XH, Iwamoto Y, Chen YW, Tong R. Multi-scale deep convolutional neural networks for emphysema classification and quantification. *Deep Learning in Healthcare: Paradigms and Applications*. 2020:149-64.
- [24] Wang Q, Zheng Y, Yang G, Jin W, Chen X, Yin Y. Multiscale rotation-invariant convolutional neural networks for lung texture classification. *IEEE journal of biomedical and health informatics*. 2017;22(1):184-95.
- [25] Anthimopoulos M, Christodoulidis S, Ebner L, Christe A, Mougiakakou S. Lung pattern classification for interstitial lung diseases using a deep convolutional neural network. *IEEE transactions on medical imaging*. 2016; 35(5):1207-16.

- [26] Ho TT, Kim T, Kim WJ, Lee CH, Chae KJ, Bak SH, Kwon SO, Jin GY, Park EK, Choi S. A 3D-CNN model with CT-based parametric response mapping for classifying COPD subjects. *Scientific Reports*. 2021;11(1):34.
- [27] Çallı E, Murphy K, Scholten ET, Schalekamp S, van Ginneken B. Explainable emphysema detection on chest radiographs with deep learning. *Plos one*. 2022;17(7):e0267539
- [28] Pisano ED, Zong S, Hemminger BM, DeLuca M, Johnston RE, Muller K, Braeuning MP, Pizer SM. Contrast limited adaptive histogram equalization image processing to improve the detection of simulated spiculations in dense mammograms. *Journal of Digital imaging*. 1998;11:193-200
- [29] Hussein F, Mughaid A, AlZu'bi S, El-Salhi SM, Abuhaija B, Abualigah L, Gandomi AH. Hybrid clahe-cnn deep neural networks for classifying lung diseases from x-ray acquisitions. *Electronics*. 2022;11(19):3075.